Acta Oceanol. Sin., 2025, Vol. 44, No. 4, P. 121–138
https://doi.org/10.1007/s13131-025-2477-1

Seasonal variation in energy flow determined by phytoplankton succession in the Ross Sea ecosystem

Hao Wei[1, 2], Yongli Zhang[1], Wei Zhao[1], Xiaofan Luo[1*], Longxing Zhu[1]

[1] Tianjin Key Laboratory for Marine Environmental Research and Service, School of Marine Science and Technology, Tianjin University, Tianjin 300072, China

[2] Laoshan Laboratory, Qingdao 266237, China

Received 14 October 2024; accepted 11 April 2025

© Chinese Society for Oceanography and Springer-Verlag GmbH Germany, part of Springer Nature 2025

Abstract

Seasonal variation in phytoplankton composition influences the pathways and efficiency of energy flow, reshaping the structure of the trophic pyramid in the Ross Sea. However, field investigation of grazing processes presents challenges that hinder our understanding of energy pathways. This study aims to provide insights into energy flow using a three-dimensional ecosystem model applied to the Ross Sea. By analyzing the simulation results, the role of the seasonal phytoplankton succession, specifically the shift from dominance by *Phaeocystis antarctica* to diatoms, in energy allocation is explored. The short-lived spring bloom of *P. antarctica* mainly fuels microzooplankton, creating a brief food chain where energy transfers primarily among smaller plankton. In contrast, the subsequent summer bloom of diatoms, which persists longer, provides nearly half of the total phytoplankton energy loss (via ingestion and mortality) to larger mesozooplankton. Our findings indicate that phytoplankton succession in the Ross Sea extends the bloom duration, particularly for diatoms, thereby facilitating energy transfer to higher trophic levels and improving overall energy utilization. This suggests that phytoplankton succession, an ecological strategy adapted to iron-deficient environments in the Ross Sea, explains why the colder region in front of the Ross Ice Shelf is significantly more productive than the northern areas, ultimately favored by top predators.

Key words energy flow, plankton ecosystem, seasonal succession, ecosystem model, Ross Sea

Citation Wei Hao, Zhang Yongli, Zhao Wei, Luo Xiaofan, Zhu Longxing. 2025. Seasonal variation in energy flow determined by phytoplankton succession in the Ross Sea ecosystem. Acta Oceanologica Sinica, 44(4): 121–138, doi: 10.1007/s13131-025-2477-1

1 Introduction

As the most productive region in the Southern Ocean (Arrigo and van Dijken, 2003), the Ross Sea provides food and habitat for a large and diverse group of top predators, such as 38% and 26% of the world's Adelie penguins and emperor penguins, respectively (Ballard et al., 2010; Smith et al., 2012). These higher trophic creatures exhibit patchy distribution, further influenced by seasonal environmental changes and the migration patterns of certain species (Thrush et al., 2006; Ballard et al., 2012; Smith et al., 2012). For example, Antarctic krill primarily inhabit near the slope, while crystal krill is found over the shelf (Sala et al., 2002; Davis et al., 2017). Penguins generally occupy the western coastal area of the Ross Sea during austral spring and migrate eastward for molting on pack ice in summer (Fig. 1a) (Davis et al., 1996; Kooyman et al., 2004; Ballard et al., 2010). As the vital food source for higher trophic levels, the temporal and spatial variations of the lower trophic levels, including phytoplankton and zooplankton, are of great scientific significance for grasping the food web structure and informing ecological protection strategies in the Ross Sea.

The dominant functional groups of phytoplankton over the Ross Sea shelf are *Phaeocystis antarctica* and the diatoms (e.g., El-Sayed et al., 1983; Smith et al., 2010; Smith, 2022). They contribute differently to the higher trophic levels (Fig. 1b). Krill primarily transfers energy to top predators by feeding on diatoms, along with some zooplankton (Pakhomov and Perissinotto, 1997; Haber-

Foundation item: The National Natural Science Foundation of China under contract No. 41941008; the National Key Research and Development Program of China under contract No. 2023YFC3107702.
*Corresponding author, E-mail: xiaofan.luo@tju.edu.cn

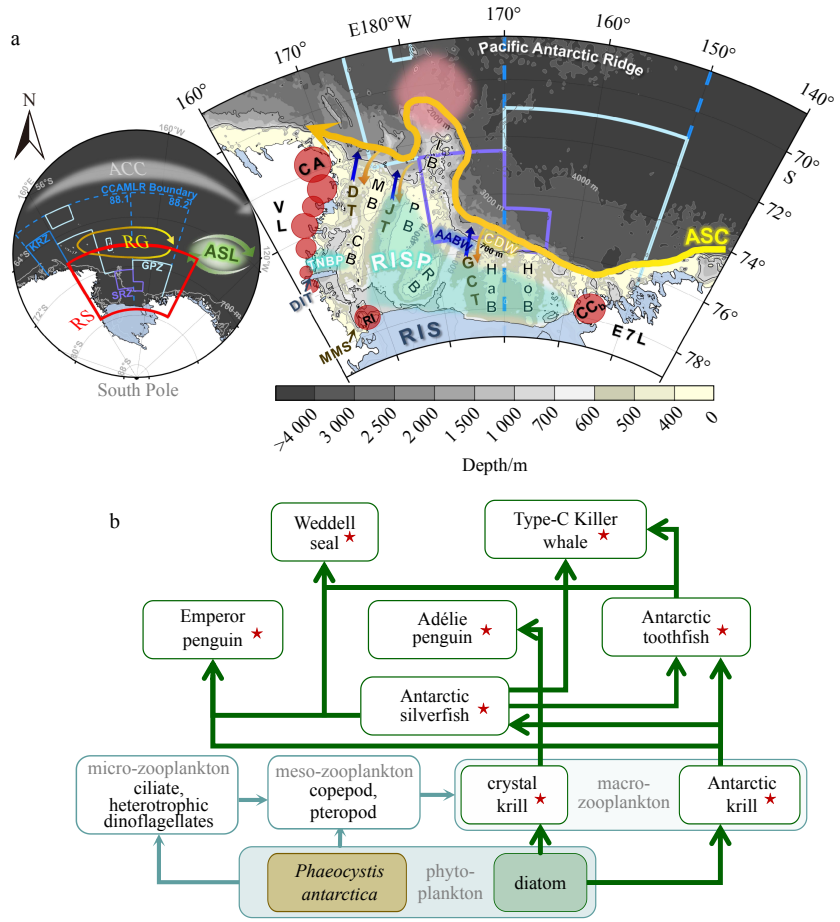


Fig. 1. Location and topography of the Ross Sea (a) with the full name of the abbreviation provided in Table A1. Flow chart of feeding relationships among major species in the Ross Sea (b) summarized from the published literatures listed in Table S1. Red stars represent indicator species in the Southern Ocean.

man et al., 2003; La et al., 2015; Schmidt et al., 2016). Meanwhile, the colony formation of *P. antarctica* is recognized as a defense mechanism against grazing (Tang et al., 2008; Ryderheim et al., 2022), with only a few types of mesozooplankton (e.g., copepods) and microzooplankton (ciliates, heterotrophic flagellates) known to ingest them (Weisse et al., 1994; Schoemann et al., 2005; Nejstgaard et al., 2007). Additionally, dead *P. antarctica* sink rapidly out of the upper water column (Mari et al., 2004; Shields and Smith, 2008). Thus, the community composition of phytoplankton and zooplankton is critical in regulating energy flow pathways and transfer efficiency in the upper water column over the Ross Sea shelf.

Primary production over the Ross Sea shelf is extremely high (Smith and Asper, 2001; Arrigo et al., 2008), characterized by a seasonal succession of dominant phytoplankton species transitioning from *P. antarctica* to diatoms (Smith et al., 1996, 2006, 2013, 2014; Peloquin and Smith, 2007; Smith and Meyer, 2020). In contrast, the biomass of mesozooplankton and microzooplankton is significantly low (Smith et al., 2007), which is suggested to be linked to trophic cascades resulting from consumption by higher trophic levels (e.g., Caron et al., 2000; Tagliabue and Arrigo, 2003). This contributes to the typical "wasp-waist" structure of the Ross Sea food web (Ainley et al., 2015). However, investigations into the abundance and feeding processes of zooplankton have been quite limited, hindering our understanding of the energy pathways between primary producers and top predators. Numerical models may provide constructive insights to address this gap.

This study first evaluates a three-dimensional coupled ocean-sea ice-ecosystem model using *in-situ* observations of chlorophyll-*a* (Chl-*a*) concentrations in surface waters. By analyzing the 10-year model hindcast simulation, we clarify the temporal and spatial evolution of phytoplankton and zooplankton in the Ross Sea, quantify the seasonal energy flow within the plankton ecosystem, and explain its connection to the distribution of higher trophic levels, elucidating why the Ross Sea shelf is recognized as a biological hotspot for top predators.

2 Data and methods

2.1 *The Ross Sea ocean-sea ice-ecosystem model*

In this study, we applied a three-dimensional coupled ocean-sea ice-ecosystem model, referred to as ROSE, to the Ross Sea (Fig. 2a). There are limited observational data on biomass, grazing rates, and grazing preferences of the Southern Ocean pelagic ecosystem. Therefore, we first

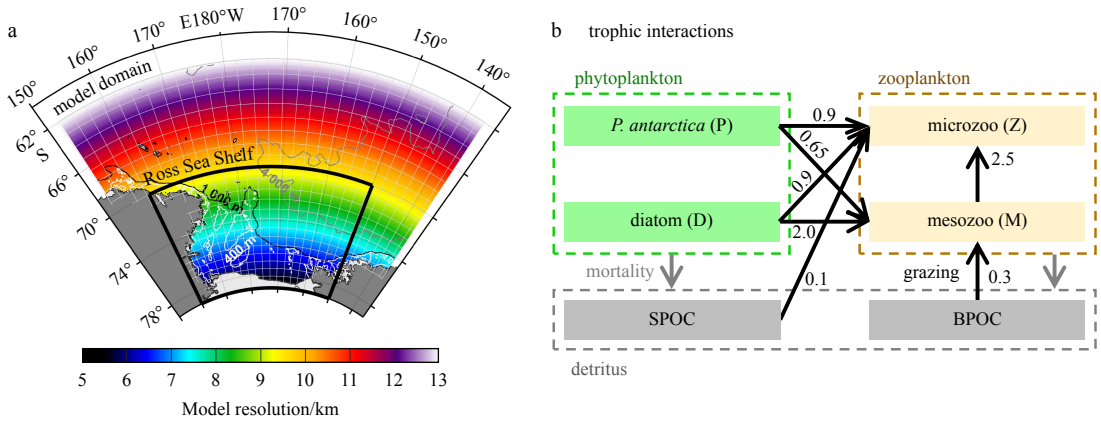


Fig. 2. Model domain, horizontal resolution of ROSE, and area of interest outlined in black box (a). Plankton structure, trophic interactions (represented by arrows), and grazing preference in ROSE (b). SPOC: small particulate organic carbon; BPOC: big particulate organic carbon.

optimized the bulk mixed layer model RISPEM (the Ross Ice Shelf polynya ecosystem model; Zhang et al., 2023b) and then coupled it with the NEMO3.6 ocean model (Madec and NEMO Ocean Engine, 2008) and the LIM3 sea ice module (Vancoppenolle et al., 2009; Rousset et al., 2015) to obtain the regional model ROSE. RISPEM was established to capture the main ecological characteristics of the Ross Sea by fine-tuning parameters related to bottom-up and top-down processes derived from the low-trophic-level ecosystem model PISCES-v2 (Aumont et al., 2015). These parameters include the phytoplankton intrinsic growth rate, iron-to-carbon ratio, grazing rate and preference, etc. (Zhang et al., 2023b). Comparisons with *in-situ* observations and published evidence indicate that RISPEM reasonably reproduces seasonal variations in total Chl-*a* and the succession of phytoplankton. Since the optimization of the parameters of RISPEM, based on 56 sensitivity experiments divided into 3 groups, has been published in the main body of Zhang et al. (2023b) and its appendixes, the design and results of sensitivity experiments that are related to grazing rate, maximum grazing rate, half constant of grazing, and grazing preferences of micro-zooplankton for *Phaeocystis* and diatoms will be described briefly hereafter.

During the stage of optimization of RISPEM, we chose daily chlorophyll observations at 77°S and 169°E near the Ross Ice Shelf (RIS) from November 22, 2012, to August 8, 2013 (Jones and Smith, 2017), as a criterion and singled out the sensitivity experiments in which the RMSE between simulation results and observed chlorophyll data was minimized. The relationship of maximum grazing rates between the micro- and meso-zooplankton was explored by setting the values of parameters to be equal or twice the other, respectively. The results of original run, experiment Nos 1–5 and 1–6 showed that the case with a grazing rate of microzooplankton twice bigger than mesozooplankton's was more realistic [see supporting information of Zhang et al. (2023b)]. On the contrary, it was confirmed that the half-saturation constants of grazing for meso-zooplankton should be higher than that of the micro-zooplankton's (experiment Nos 1–7 and 1–8), implying a greater appetite of the former functional group. Then, the optimal values of the above parameters were determined by a series of experiments (experiment Nos 2–17 to 2–22). More importantly, Zhang et al. (2023b) demonstrated through sensitivity experiments that microzooplankton feeding on *Phaeocystis* was indispensable for the formation of seasonal species succession in which *Phaeocystis* was replaced by diatoms in austral summer, and that there was a possibility that microzooplankton preferred to feed on *Phaeocystis* (control run, experiment No. D14–16).

ROSE contains 24 prognostic ecological variables to describe the lower trophic levels of the Ross Sea, including two types of phytoplankton (*P. antarctica* and diatoms) and two types of zooplankton (microzooplankton and mesozooplankton). Key processes modeled include photosynthesis, respiration, zooplankton grazing on phytoplankton, and death of zooplankton. Grazing preferences of zooplankton are illustrated in Fig. 2b. Mesozooplankton in ROSE represents copepods and crystal krill (Pakhomov and Perissinotto, 1997), which share similar food sources, primarily feeding on diatoms, while also consuming ciliates (microzooplankton) and *P. antarctica*. It is worth mentioning that bacteria, as an implicit variable, participate in the decomposition of organic matter and also consume nutrients, as detailed in Aumont et al. (2015). Due to the fact that bacteria do not directly participate in the feeding process of planktonic ecosystems, they are not included in the concept diagram (Fig. 2b).

The model domain of ROSE encompasses the area south of 62°S, from 152°E to 137°W, covering the entire Ross Sea Shelf (Fig. 2a). It features a nominal horizontal resolution of (1/4)° in latitude/longitude with 75 vertical levels. Details regarding forcing fields, initial conditions, and open boundary conditions are provided in Table S2. Multi-year averages of ROSE hindcast simulations from July 2010 to June 2020 are used for analysis.

2.2 *Model evaluation*

The MODIS satellite-based Chl-*a* product, using the

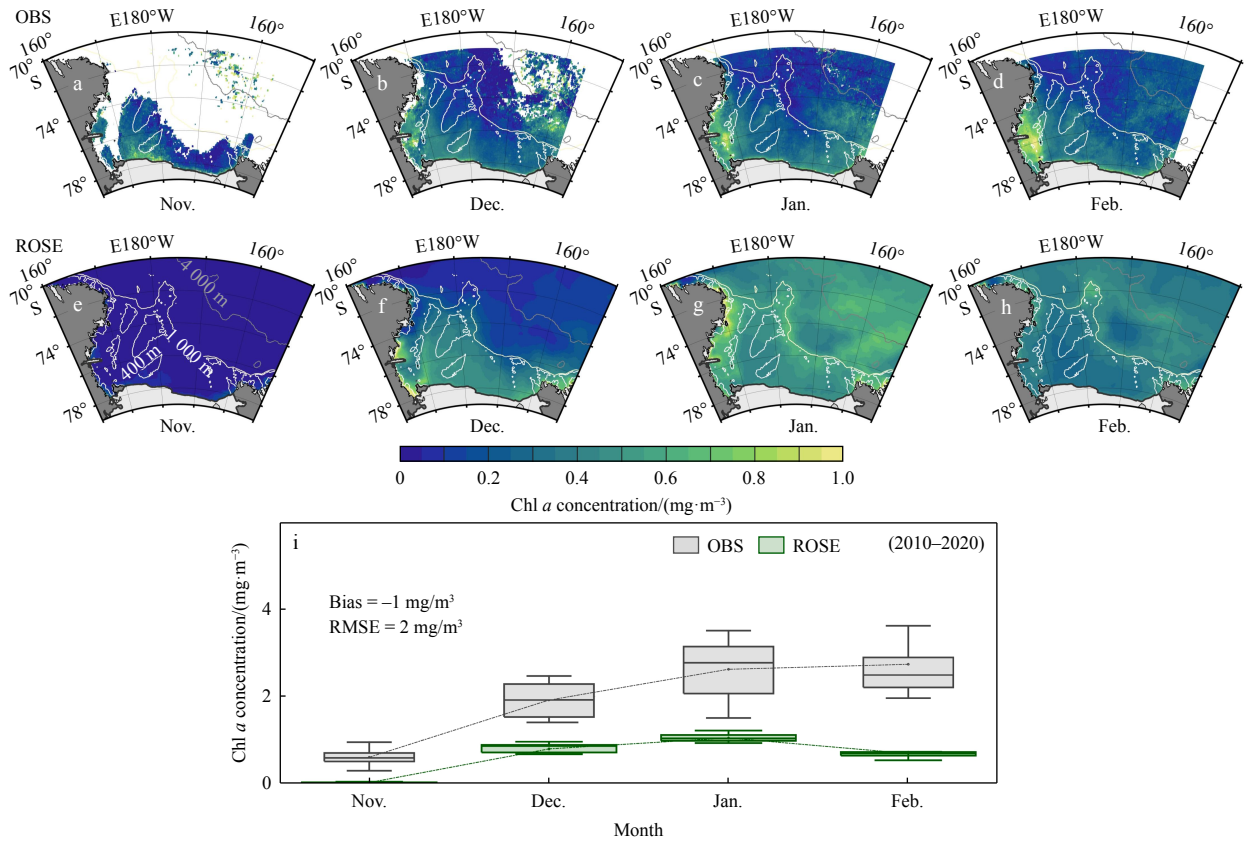


Fig. 3. Spatial distribution of normalized satellite-based (a–d) and ROSE simulated (e–h) Chl *a* concentration ($\mathrm{Chl}^{X}_{\mathrm{NRM}}$) at the surface over the Ross Sea Shelf averaged from November 2010 to February 2020 and their monthly time series (i).

Rrs667 algorithm developed by Chen et al. (2021), hereinafter referred to as Rrs667, was selected for model evaluation. First, the monthly Rrs667 observations averaged over 2010–2020 were interpolated into the ROSE model grid. Due to persistent cloud cover reducing the spatial continuity of satellite observations (e.g., Figs 3a and b), we counted the grids with available observations each month and compared these with model simulations from the same grids at the corresponding times. The Rrs667 observation and ROSE simulated results were then processed separately to obtain normalized Chl-*a* concentration ($\mathrm{Chl}^{X}_{\mathrm{NRM}}$, NRM refers to normalized), as shown in Eq. (1):

$$\mathrm{Chl}^{X}_{\mathrm{NRM}} = \frac{\mathrm{Chl}^{X} - \min\left(\mathrm{Chl}^{X}\right)}{\max\left(\mathrm{Chl}^{X}\right) - \min\left(\mathrm{Chl}^{X}\right)}, \tag{1}$$

where X denotes either the Rrs667 observation or the ROSE simulation.

Both the normalized Rrs667 and ROSE indicate that phytoplankton biomass initially forms and then expands in the Ross Ice Shelf polynya (RISP) and the Terra Nova Bay polynya (TNBP) from November, although ROSE slightly underestimates the surface Chl-*a* concentration (Figs 3a and e). In December, normalized Rrs667 shows that Chl-*a* over the western shelf is higher in the south than in the north, a pattern that ROSE captures well (Figs 3b and f). This south-north Chl-*a* gradient intensifies in January and February, according to normalized Rrs667 (Figs 3c and d), while ROSE presents high Chl-*a* levels over the western slope and Iselin Bank (IB) (Figs 3g and h), consistent with recent observed findings (Cristi et al., 2024).

ROSE also reasonably reproduces the rapid increase of Chl-*a* starting in November (Fig. 3i). After peaking in January, simulated Chl-*a* decreased in February, showing a similar seasonal growth rate to the normalized Rrs667 observations. The bias and RMSE between Rrs667 observed and ROSE simulated surface Chl-*a* concentrations are obtained as –1 mg/m^3 and 2 mg/m^3, respectively. Evaluations of ROSE simulated sea ice concentration, macronutrients and dissolved iron concentration can be found in Zhang (2024). Overall, ROSE demonstrates a reasonable skill in reproducing the seasonal cycle and spatial gradient of the plankton ecosystem over the Ross Sea shelf from 2010 to 2020, paving the way for further analysis.

2.3 *Implications of specific indicators*

The onset and end dates of phytoplankton growth are defined as the dates when the total Chl-*a* of *P. antarctica* and diatoms first and last reaches 5% of their annual max-

imum, respectively. The date of Seasonal Species Succession is marked by the point at which the biomass of *P. antarctica* and diatoms becomes equal. Accordingly, the total duration of blooms is categorized into the dominant stages of *P. antarctica* and diatoms, referred to as P-period and D-period. Statistical measures of mean and standard deviation are used to assess the variation of a given state variable within the Ross Sea ecosystem. The ratio of standard deviation to mean is further defined as the "degree of variation", serving to quantify regional differences.

Total particulate organic carbon (POC) encompasses the living POC of phytoplankton and zooplankton, as well as non-living POC. According to Lindeman Efficiency (Lindeman, 1942), the total energy loss of phytoplankton, including ingestion and mortality, is considered equivalent to the total available energy generated by primary production that supports the higher trophic levels. By estimating the ratio of carbon content in various forms (including *P. antarctica*, diatoms, microzooplankton, mesozooplankton, small POC, and large POC) to the total phytoplankton loss, the energy flow pathways within the plankton ecosystem are characterized.

3 Results and discussions

3.1 *Temporal and spatial variations in phytoplankton and zooplankton biomass*

The ROSE simulation indicates a clear seasonal species succession, highlighted by *P. antarctica* and diatom biomass within the upper 100 m over the Ross Sea shelf averaged over 2010–2020 (Fig. 4a). The *P. antarctica* bloom begins on November 7 and peaks on December 16, followed by a rapid decline starting in early January. The diatom bloom occurs in early December, with biomass remaining at approximately 200 mmol/(m^2·d) (in terms of C) in January. By mid-February, diatom biomass gradually decreases until it ends in mid-April. The biomass of *P. antarctica* and diatoms are found to be equal on December 23, marking the point of seasonal succession of phytoplankton species. These simulated patterns align closely with multi-year observations (Smith et al., 2014).

Comparing the P-period and D-period, the ROSE simulation reveals that the dominant stage of diatoms (from December 23 to April 17) lasts 2.5 times longer than that

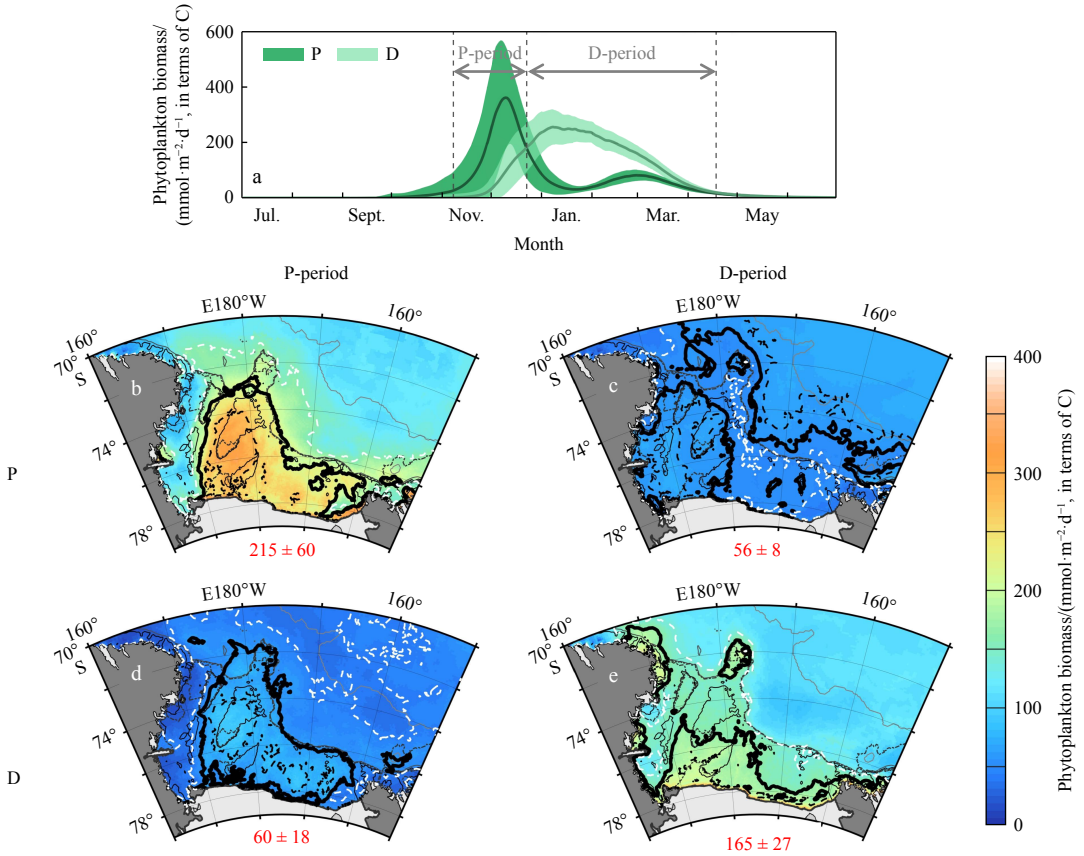


Fig. 4. Daily time series (a) and spatial distributions (b–e) of phytoplankton biomass in the upper 100 m layer averaged from 2010 to 2020. In a, the solid dark green and light green lines represent the mean biomass of *Phaeocystis antarctica* (P) and diatoms (D), respectively, for the interested area, with the corresponding color bands denoting spatial standard deviation. Gray dashed lines mark the onset date, the point of seasonal species succession, and the end of the bloom. b–e illustrate the spatial distribution of mean biomass for P and D during the P-period and D-period, with the mean biomass indicated by solid black curves and the mean biomass ± standard deviation shown by dotted black and white curves. Red numbers below each sub-figure represent the mean biomass ± standard deviation [mmol/(m^2·d), in terms of C].

of *P. antarctica* (November 7 to December 23). But the annual peak biomass of *P. antarctica* is 1.5 times greater than that of diatoms. During the P-period, the average biomass of *P. antarctica* is approximately four times that of diatoms. The higher biomass of *P. antarctica* is primarily found in TNBP and RISP, covering most of the western shelf from the front of the RIS to the slope (Fig. 4b). As diatoms gain dominance, the region of higher diatom biomass retreats southward to the front of RIS (Fig. 4e). Throughout the bloom, total phytoplankton biomass over the shelf is noticeably higher than that in the slope and northern basin. The spatial standard deviation of biomass shows that *P. antarctica* exhibits the greatest variability during its dominant period (dark green band in Fig. 4a), with a standard deviation-to-mean ratio of 28% (28% = 60/215; Fig. 4b). This ratio is higher than that for diatom biomass during the D-period, which is 16% (16% = 27/165; Fig. 4d), further suggesting a greater regional variability of *P. antarctica* compared to diatoms in the Ross Sea.

The seasonal succession of zooplankton begins on January 31, following a 38-d lag after phytoplankton succession (Fig. 5a). The biomass of microzooplankton rapidly increases (solid blue line in Fig. 5a) during the P-period, peaking at approximately 200 mmol/(m^2·d) (in terms of C) in early January. This peak is higher than that of mesozooplankton (solid purple line in Fig. 5a) but lower than that of *P. antarctica* (Fig. 4a, dark green solid line). By early February, microzooplankton biomass declines to about half of its annual peak, reaching a level roughly equal to the highest biomass of mesozooplankton. Mesozooplankton then remains dominant until the end of the bloom.

Overall, the spatial variability in microzooplankton biomass is greater than that of mesozooplankton, as indicated by their spatial standard deviation (blue and purple bands in Fig. 5a). During the P-period, microzooplankton exhibit higher biomass over the shelf compared to the northern basin (Fig. 5b), while mesozooplankton shows a more uniform distribution with lower biomass (Fig. 5d). During the D-period, both microzooplankton and mesozooplankton thrive near the front of the RIS, mirroring the distribution of phytoplankton. In contrast, the total biomass of zooplankton remains notably low along the

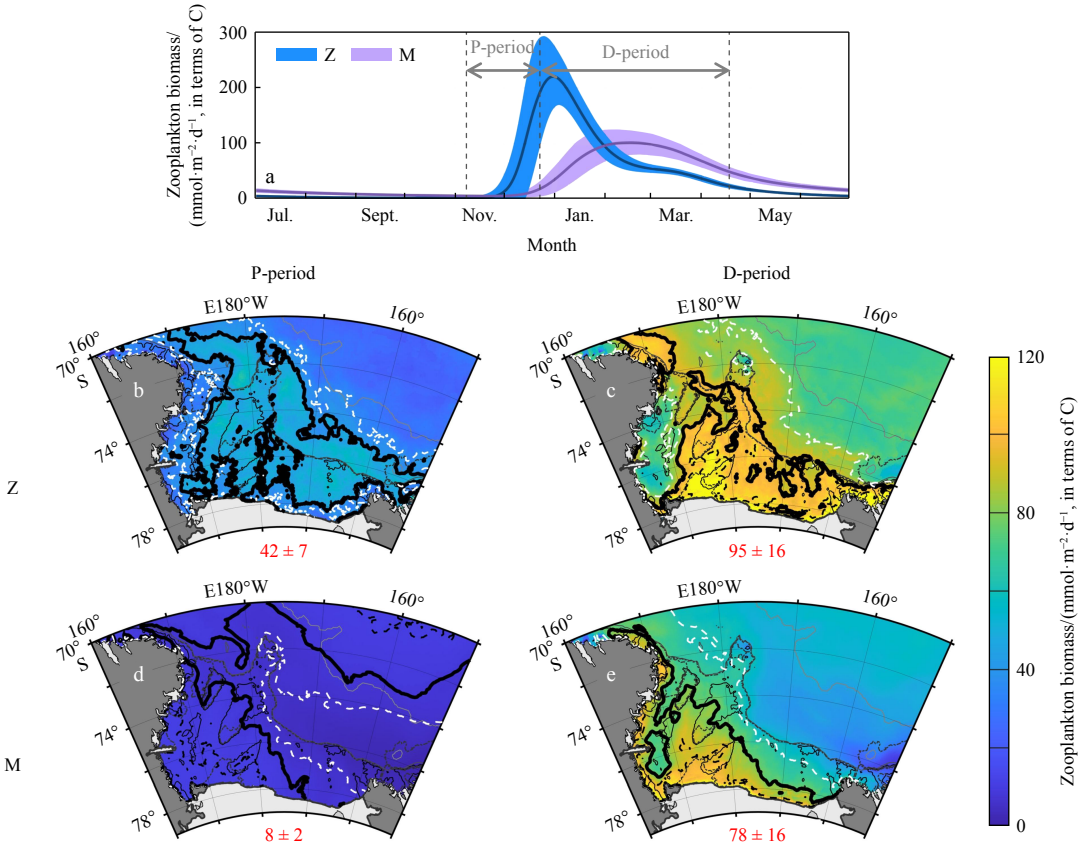


Fig. 5. Daily time series (a) and spatial distributions (b–e) of zooplankton biomass in the upper 100 m layer averaged from 2010 to 2020. In a, the solid blue and purple lines represent the mean biomass of microzooplankton (Z) and mesozooplankton (M), respectively, for the interested area, with the corresponding color bands denoting spatial standard deviation. Gray dashed lines mark the onset date of phytoplankton bloom, the point of seasonal phytoplankton species succession, and the end of the bloom. b–e illustrate the spatial distribution of mean biomass for Z and M during the P-period and D-period, with the mean biomass indicated by solid black curves and the mean biomass ± standard deviation shown by dotted black and white curves. Red numbers below each sub-figure represent the mean biomass ± standard deviation [mmol/(m^2·d), in terms of C].

Victoria Land coast over the western shelf throughout the phytoplankton growth period.

3.2 *Controls on the spatio-temporal variations in primary production*

Primary production (PP) serves as the energy source for zooplankton and virtually the entire trophic pyramid (Woodward, 2007). The ROSE simulation reveals that the spatio-temporal characteristics of PP (Figs 6b–f) in the Ross Sea closely align with phytoplankton biomass (Figs 4a–e). Notably, significant environmental differences exist during the dominant periods of *P. antarctica* and diatoms. Sea ice undergoes marked seasonal changes (Fig. 6a); in austral winter, the average sea ice thickness (SIT) is about 1 m, gradually decreasing from late October. During the P-period, sea ice loss accelerates, with daily SIT declines reaching up to 1 cm (Fig. 6a). By the start of D-period, the average SIT drops to around 0.2 m and remains stable until the phytoplankton bloom ends.

A comparison of the spatial distribution of SIT and PP during the P-period shows that higher PP is associated with SIT thinner than 0.4 m (Fig. 6c), indicating that polynyas like RISP and TNBP are hot spots for *P. antarctica*. Previous studies have shown that light penetration in surface waters decreases exponentially with increasing SIT, with a 1-m increase in SIT resulting in a 95%–99% reduction in shortwave radiation (Katlein et al., 2016; Arndt et al., 2017). Thus, the relatively lower SIT facilitates stronger photosynthetically active radiation (PAR), allowing RISP and TNBP to present high biomass of *P. antarctica* by mid-December. During the D-period, open water areas rapidly expand northward, reducing the ice-induced light limitation on phytoplankton growth in the Ross Sea. Overall, the spatial variability of diatom-contributed primary production during D-period is much less than that of *P. antarctica* during the P-period.

In addition to light limitation, iron availability significantly influences the spatial and temporal evolution of PP. Since the onset of bloom in November, dissolved iron (dFe) in the upper water column has been rapidly depleted, leading both phytoplankton species to grow under iron-limited conditions. The solid and dashed lines in Fig. 7a

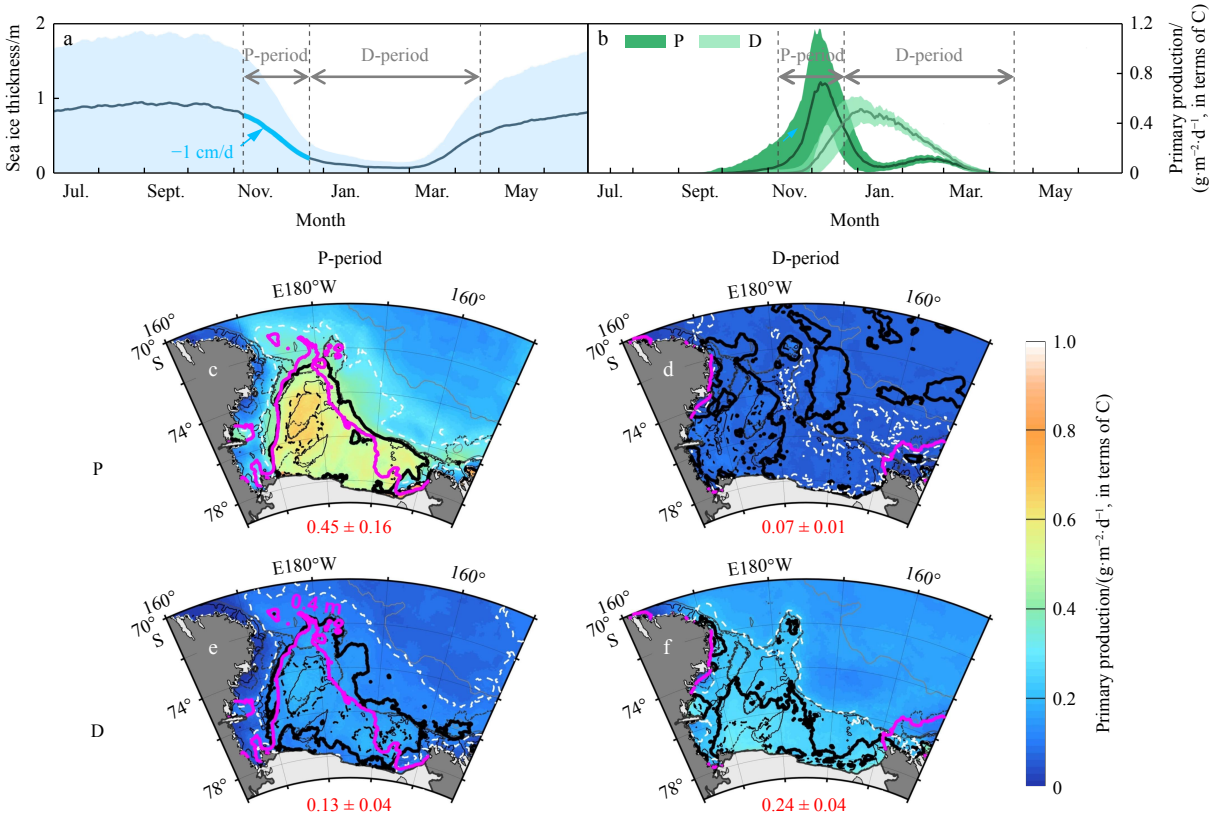


Fig. 6. Daily time series of sea ice thickness (a). b–f show daily time series (b) and spatial distributions (c–f) of primary production in the upper 100 m layer averaged from 2010 to 2020. In b, the solid dark green and light green lines represent the mean primary production contributed by *P. antarctica* (P) and diatoms (D), respectively, for the interested area, with the corresponding color bands denoting spatial standard deviation. Gray dashed lines mark the onset date of phytoplankton bloom, the point of seasonal phytoplankton species succession, and the end of the bloom. c–f illustrate the spatial distribution of mean primary production contributed by P and D during the P-period and D-period, with the mean value indicated by solid black curves and the mean value ± standard deviation shown by dotted black and white curves. Red numbers below each sub-figure represent the mean value ± standard deviation [g/(m^2·d), in terms of C]. Magenta contours in c–f indicate SIT of 0.4 m.

illustrate the daily variations in iron limitation on *P. antarctica* and diatoms simulated by ROSE. Throughout the growing season, iron limitation is consistently stronger for *P. antarctica* than for diatoms, indicating a relatively high iron requirement for *P. antarctica* growth, consistent with previous findings (Coale et al., 2003; Sedwick et al., 2007; Strzepek et al., 2012; Kustka et al., 2015; Wu et al., 2019; McCain et al., 2022; Zhang et al., 2023b). Notably, Pennell Bank, located over the middle shelf, experiences more severe iron limitation during the D-period, which inhibits diatom growth (Figs 7c and e). This occurs because *P. antarctica* depletes dFe in the upper layer during the P-period. Additionally, the D-period possesses substantial regional differences in iron limitation across open water areas (where light limitation is minimal), suggesting that iron limitation will amplify the spatial variability of PP, especially during the later phytoplankton season.

3.3 *Seasonal variations in energy flow of plankton ecosystem*

Seasonal variations in zooplankton feeding behaviors are analyzed to clarify characteristics of energy transfer efficiency within the plankton ecosystem in the Ross Sea (Fig. 8). During the P-period, microzooplankton (Z) obtains 59.2% of the total energy loss of *P. antarctica* and diatoms, which is 6.8 times the total energy obtained by mesozooplankton (M). In this period, P serves as the main food source for Z, contributing 75% (44.4% of 59.2%), followed by small POC (SPOC) at 24% (14.4% of 59.2%) (Figs 8a and c). Considering that the mortality and subsequent sinking of P also contribute to the formation of SPOC, the spatial patterns of Z biomass (Fig. 5c) and its food intake (Figs 9a and b) (low over the western shelf but high over the central shelf) are largely determined by the spatial distribution of PP (Figs 6c and e). Energy transferred from Z to M through grazing constitutes 0.8% of the total energy loss of phytoplankton, roughly one-tenth of the energy obtained by M directly ingesting phytoplankton and POC (7.9%). Additionally, the contribution of P to SPOC due to mortality and subsequent sinking is notable at 29.3%. The carbon content percentages in total POC are 37% for P, 37% for SPOM, and 9% for Z. These findings indicate that the spring bloom of P triggers the majority of energy transfer in the short food chain among small plankton (from P to Z) and to SPOC in the upper layer.

When D dominates, there is a notable shift in energy transfer patterns within plankton ecosystems. D becomes the primary contributor to PP, supplying 78% of the total energy to the ecosystem (Fig. 8d). The percentage of

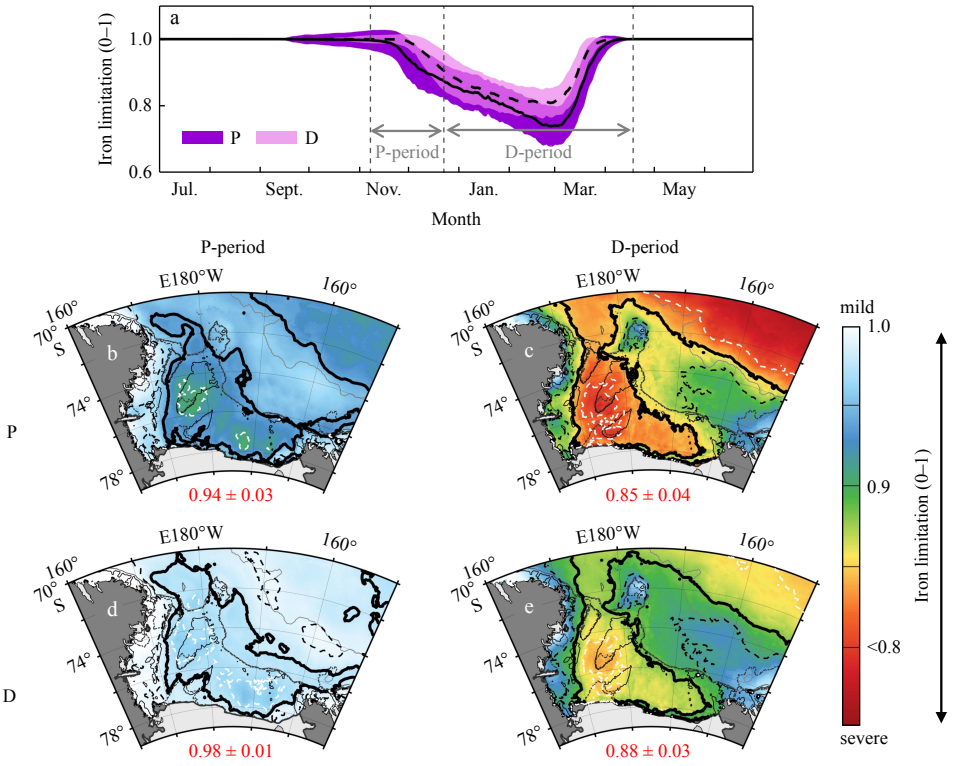


Fig. 7. Daily time series (a) and spatial distributions (b–e) of iron limitation on phytoplankton growth. In a, the solid and dashed black lines represent the mean value of iron limitation on *P. antarctica* (P) and diatoms (D), respectively, for the interested area, with the color bands denoting spatial standard deviation. Gray dashed lines mark the onset date of phytoplankton bloom, the point of seasonal phytoplankton species succession, and the end of the bloom. b–e illustrate the spatial distribution of iron limitation on P and D during the P-period and D-period, with the mean value indicated by solid black curves and the mean value ± standard deviation shown by dotted black and white curves. Red numbers below each sub-figure represent the mean value ± standard deviation.

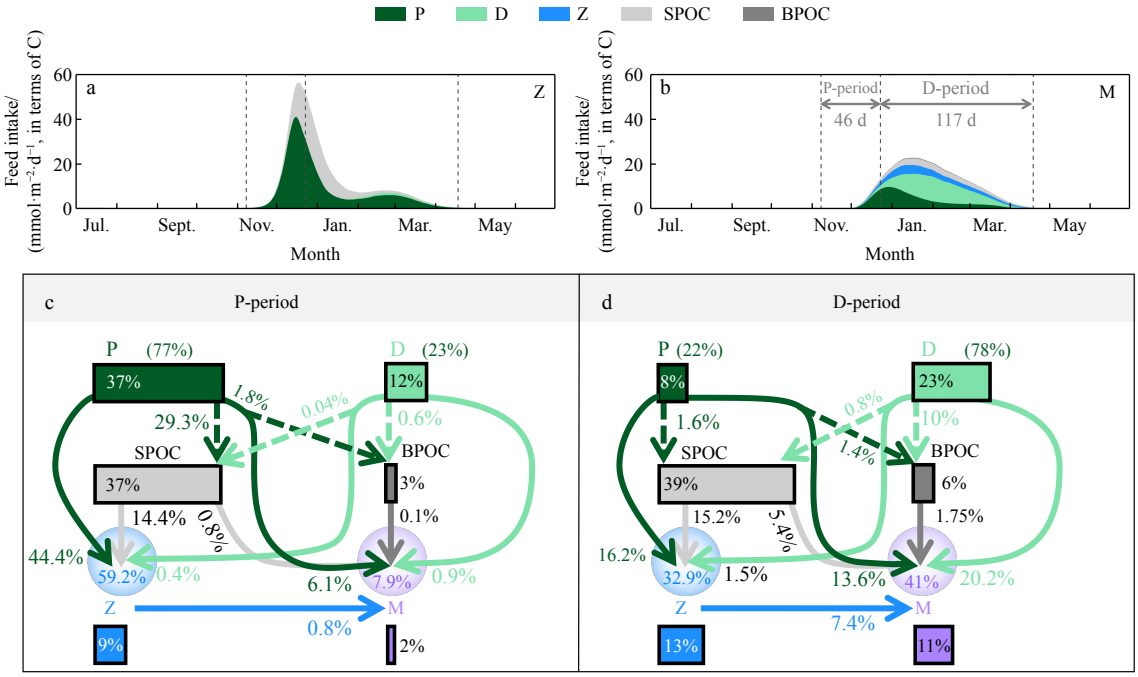


Fig. 8. Daily time series of feed intakes of microzooplankton (a) and mesozooplankton (b), and energy flow during P-period (c) and D-period (d). In a and b, shading represents the following: dark green for zooplankton directly feeding on *Phaeocystis antarctica* (P), light green for diatoms (D), blue for microzooplankton (Z), light gray for small particulate organic carbon (SPOC), and dark gray for big particulate organic carbon (BPOC). In c and d, purple boxes denote mesozooplankton (M), while other colored boxes correspond to the indicator with matching shades from a and b. Percentages in parentheses indicate the contribution of *Phaeocystis antarctica* and diatoms to total primary production. Percentages within or near the boxes represent the ratio of carbon content to total POC. Percentages next to solid arrows denote the energy ratio obtained by zooplankton in various ways relative to the total phytoplankton energy loss, whereas percentages next to dashed arrows denote the energy that remained in non-living POC, contributing to the total phytoplankton energy.

20.2% in the total energy is directly transferred to M through feeding, making it the main food source for M, while P and Z contribute 13.6% and 7.4%, respectively (Figs 8b and d). The spatial distribution of M's feeding on D presents greater variability than that on P, with standard deviation-to-mean ratios of 26.8% and 20.5% (Figs 9e and f). The former feeding distribution closely aligns with the spatial patterns of M biomass (Fig. 5e) and D-contributed PP (Fig. 6f), indicating D's critical role in supporting M growth and its regional differences in the Ross Sea. During the D-period, energy transferred to M significantly exceeds that to Z, with energy capturing rates of 48.4% and 32.9% of the total energy loss of phytoplankton, respectively. Additionally, energy transfer from Z to M through grazing rises up to 7.8%, further suggesting more energy accumulation at higher trophic levels. Consequently, carbon content in M accounts for 9% of total POC, surpassing the 2% estimated in the P-period.

Energy flow pathways during P- and D-periods reveal that the P bloom tends to trigger energy flow among smaller plankton, benefiting Z in spring. The lack of iron in summer and Z's feeding on P allows D to establish dominance (Zhang et al., 2023b), facilitating energy transfer to higher trophic levels. Although D's biomass and annual peak of PP are visibly lower than those of P, D's growth season lasts over three months, providing energy to the ecosystem in a more stable manner compared to the thriving yet shorter-lived P. What would the pattern of energy transfer look like if phytoplankton community succession did not occur in the Ross Sea? If iron limitation was absent, it would favor the growth of P but hinder D from replacing P and dominating in the summer. Conversely, if iron limitation were too severe in early spring, it would impede the flourishing of P and shorten D's growth season. These two scenarios were tested through sensitivity numerical experiments in our previous study (Zhang et al., 2023b). In such cases, energy transfer from PP to top predators would be inhibited during the summer months. This suggests that the transfer efficiency to higher trophic levels benefits from the succession of phytoplankton.

3.4 *Linking plankton hotspot to top predator habitats*

According to ROSE simulations, RISP is a biological hotspot for plankton ecosystems (Figs 10a and b). Multi-year observations indicate that RISP supports over 50% of Antarctic silverfish over shelf (red squares in Fig. 10c) (Pinkerton et al., 2013) as well as large numbers of crystal krill (Davis et al., 2017), penguins (blue circles in Fig. 10c; Kooyman et al., 2004), and seals (Goetz, 2015).

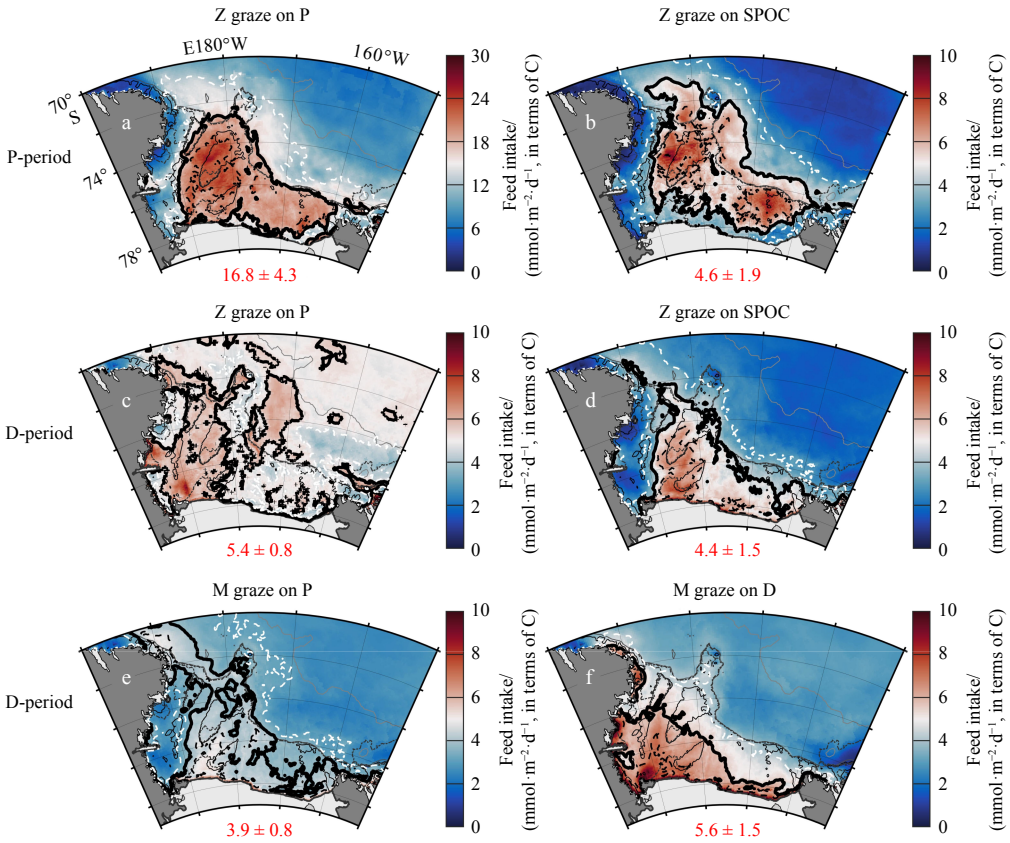


Fig. 9. Feeding distribution during P-period (a–b) and D-period (c–f). P, D, Z, M, and SPOC represent *Phaeocystis antarctica*, diatom, microzooplankton, mesozooplankton, and small particulate organic carbon, respectively. The mean value of feed intake is indicated by solid black curve and the mean value ± standard deviation are shown by dotted black and white curves. Red numbers below each sub-figure represent the mean value ± standard deviation [mmol/(m^2·d), in terms of C].

In summer, killer whales migrate through the Drygalski Trough (DT) to the RIS front (green arrow in Fig. 10c) (Ainley et al., 2012), making RISP a major feeding ground for top predators. As the main biological hotspot in the Ross Sea, RISP has diverse pathways for energy transfer to higher trophic levels. Zooplankton, key secondary producers, provides an important pathway for transferring material and energy from primary producers (phytoplankton) to higher trophic levels (Atkinson et al., 2012; Kerkar et al., 2022). However, the feeding preferences of mesozooplankton and microzooplankton for *P. antarctica* and diatoms remain uncertain, challenging a deeper understanding of the plankton ecosystem in the Ross Sea. Despite evidence of *P. antarctica* being directly consumed by macro- and mesozooplankton (e.g., Nejstgaard et al., 2007; Elliott et al., 2009; Smith et al., 2017), diatoms are still the preferred food sources for krill and copepods (e.g., Hansen and van Boekel, 1991; Haberman et al., 2003; Cleary et al., 2018).

Through a series of sensitivity experiments using the box ecosystem model RISPEM, our pervious study established reasonable feeding preference parameters for zooplankton (Zhang et al., 2023b). This study further suggested that the cascade feeding of mesozooplankton on both phytoplankton and microzooplankton, along with microzooplankton feeding on phytoplankton, creates uneven grazing pressure on different primary producers. Combined with iron limitation, this dynamic contributes to the seasonal succession of phytoplankton species, highlighting the importance of the coupling effect of top-down and bottom-up processes.

Using the same feeding preference parameters, the three-dimensional ROSE model further reveals the seasonal evolution of energy transfer within the plankton ecosystem. The seasonal succession from *P. antarctica* to diatoms is not only a response to the iron-deficient condition but also represents an ecological strategy to extend phytoplankton growth during summer and enhance energy transfer to higher trophic levels through mesozooplankton, including copepods, ice krill, etc., thereby increasing the energy transfer efficiency of the local trophic pyramid (Fig. 10d). Faced with limited zooplankton observations, the ROSE model provides quantitative insights into the relationship between phytoplankton and top predators within the energy flow of the Ross Sea.

4 Advantages and limitations of regional ecosystem model

The strengths and limitations of the regional ecosys-

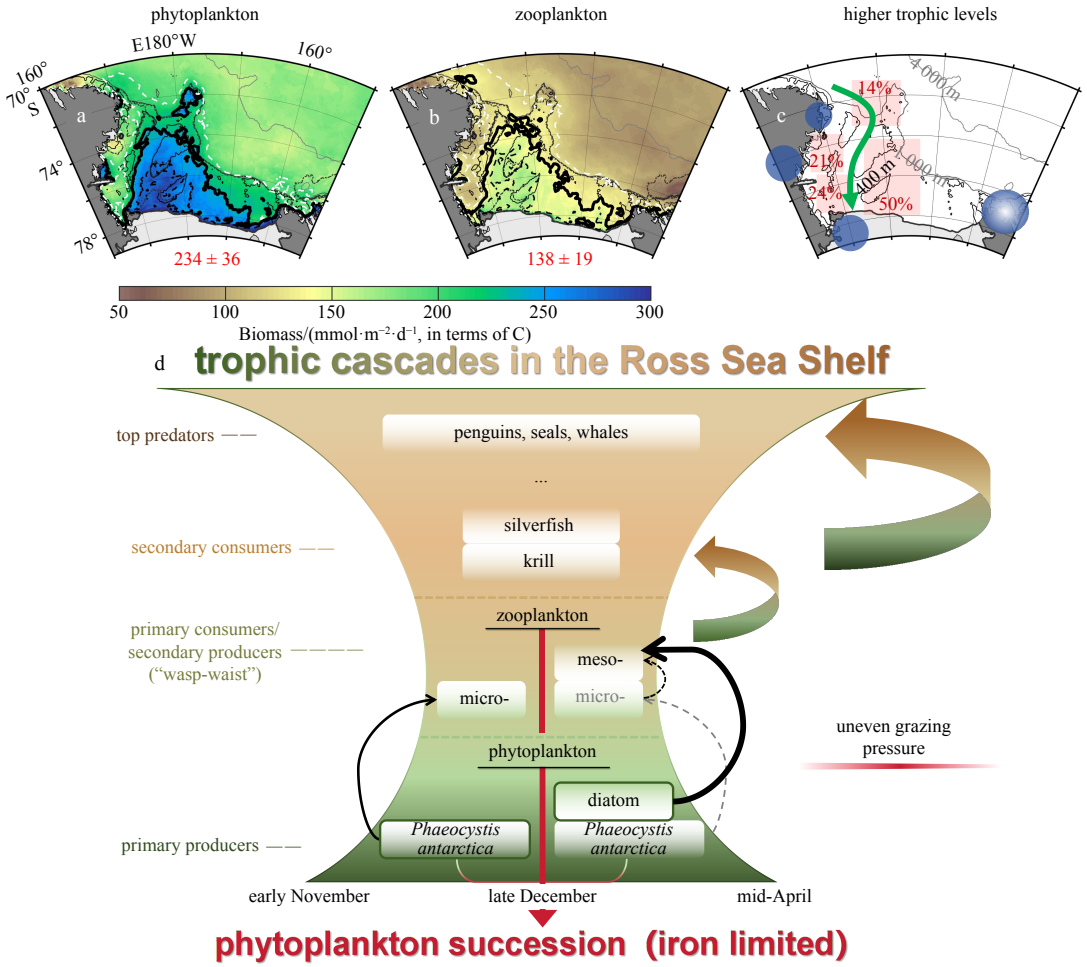


Fig. 10. ROSE simulated spatial distribution of the annual biomass of total phytoplankton (a) and zooplankton (b) in the upper 100 m layer averaged over 2010–2020, along with habitats and migration paths of top predators based on observations (c), including the location of biological hotspots for Antarctic silverfish (red squares with percentages) (Pinkerton et al., 2013), penguins (blue circles) (Kooyman et al., 2004), and migration path of killer whale (green arrow) (Ainley et al., 2012). In a and b, solid black curve indicates the mean biomass, and dotted black and white curves indicate the mean value ± standard deviation listed below in red [mmol/(m^2·d), in terms of C]. Conceptual model of the seasonal trophic cascade effects in the Ross Sea (d).

tem model ROSE will be discussed from three perspectives: ecosystem complexity, response to external environmental changes, and representativeness of ecosystem characteristics, with a particular focus on its ability to simulate and analyze energy flow within the plankton ecosystem.

4.1 *Simulation simplicity and ecosystem complexity*

Functioning as a mosaic, the Ross Sea Shelf comprises distinct ecological subsystems with notable spatial-temporal variability. Such diversity is driven by the rich variety of plankton communities, with a total of 48 taxa identified, corresponding to 27 species and 20 genera during a fortnight-long voyage on the shelf (Monti-Birkenmeier et al., 2024). Overall, microzooplankton was comprised of five main groups, with heterotrophic dinoflagellates and tintinnids being the most dominant, the latter of which was the predominant group within the ciliate community. The two major polynyas in the Ross Sea exhibited distinct planktonic sub-ecosystems. In TNBP, diatoms and heterotrophic dinoflagellates dominated the phytoplankton and microzooplankton communities, respectively. Meanwhile, in RISP, *P. antarctica* and diatoms were equally abundant, with tintinnids as the dominant microzooplankton. Despite differences in functional traits between the two microzooplankton groups, such as lorica oral diameter (LOD) of tintinnids and prey size classes, the total carbon content in the two polynyas was remarkably similar, with both exhibiting characteristics of energy transfer from phytoplankton to higher trophic levels via zooplankton, which was consistent with previous works (e.g., Steinberg and Landry, 2017; Christaki et al., 2021).

In terms of phytoplankton, *P. antarctica* and diatoms are the dominant groups, typically accounting for over 90% of the total chlorophyll (Ge et al., 2024). In contrast, dinoflagellates and cryptophytes also occur over the shelf

but are generally found most in isolated locations (Leventer and Dunbar, 1996; Arrigo et al., 1999; Smith et al., 2012). Therefore, this mosaic pattern can still be distilled into a unified framework. Firstly, using the zero-dimensional ecological model RISP (Zhang et al., 2023b) and the three-dimensional regional model ROSE (this study), we discussed the general characteristics of the Ross Sea and focused on the seasonal variation of energy flow, with each functional group contributing to the balance of the ecosystem. The ROSE model demonstrates significant advantages in simulating complex ecosystems, such as its high spatial-temporal resolution and ability to couple multiple processes (physical, chemical, and biological).

Moreover, the model's flexibility in parameterizing species complexity, ranging from simplified functional groups to highly resolved subdivisions, can be transformed from a potential limitation into a strength. For instance, should microzooplankton be further subdivided into heterotrophic dinoflagellates and tintinnids to reflect their distinct prey preferences? If so, how should the parameters for their feeding dynamics be determined? These questions can be addressed through detailed sensitivity experiments, which would not only improve model accuracy but also compensate for the limitations of *in-situ* observations, such as the fragmented nature of observational time series and the temporal lag between microzooplankton biomass and grazing pressure. Additionally, while the current study focuses on the process of *P. antarctica* sinking and subsequent bacterial decomposition, the role of small consumers, such as heterotrophic nano-flagellates feeding on bacteria (Monti-Birkenmeier et al., 2024), should also be incorporated to provide a more comprehensive representation of the simulated food chain. Leveraging the spatiotemporal continuity of regional models, their simulation results can be used to explore internal ecosystem dynamics, thereby providing a more comprehensive understanding of the Southern Ocean ecosystem. In future work, we will further explore the influence of ecosystem complexity on the composition and energy flow of planktonic ecosystems.

4.2 *Response of simulations to external environment*

Given the high latitude of the Ross Sea and the consequent shortness of the light season (Ryan-Keogh and Smith, 2021), the specific processes by which external environmental factors stimulate and constrain the shelf ecosystem have become even more perplexing. In fact, processes driven by environmental factors, such as the gradual increase in light availability (e.g., Smith and Comiso, 2008; Hague and Vichi, 2021), changes in mixed layer stability (e.g., Smith et al., 2014; Ge et al., 2024), and rapid depletion of dissolved iron (e.g., Sedwick et al., 2011; Wu et al., 2019), have long been regarded as the primary factors influencing phytoplankton community structure and primary productivity. Based on extensive previous research on iron limitation of algal growth (Coale et al., 2003; Sedwick et al., 2007; Strzepek et al., 2012; Kustka et al., 2015), Zhang et al. (2023b) were the first to simultaneously emphasize the indispensable roles of both bottom-up and top-down processes in shaping the seasonal succession of phytoplankton. Zhang (2024) emphasized the regulatory role of polynya formation in early spring on light conditions, which significantly affects the spatial distribution differences in *Phaeocystis* blooms. Notably, we also specifically highlighted the influence of advection processes on the spatial patterns of POC, demonstrating that lateral POC advection significantly amplifies spatial variations in biological carbon pump efficiency, while remineralization plays a minimal role. It has been further confirmed that, under summer stratification conditions, near-inertial processes driven by intermittent strong wind events facilitate the cross-isopycnal transport of deep dissolved iron (Zhang et al., 2023a).

The ROSE model demonstrates both strengths and limitations in reflecting the influence of external environmental factors on energy flow. Its high spatial-temporal resolution and ability to couple ocean, sea ice, and ecosystem processes allow for a detailed exploration of environmental controls on energy flow dynamics. For instance, the model well reproduces the spatial and temporal variability in sea ice concentration, the evolution of coastal polynyas, and the distribution of dissolved iron and Chl-*a* levels (Zhang, 2024). These capabilities enable the model to capture key environmental driving factors, such as the availability of light regulated by sea ice, mixed layer stability, and lateral/vertical transport of nutrients, which significantly affect primary productivity and phytoplankton community structure, thereby impacting phytoplankton primary production. Numerous ecological modeling studies have been conducted to explore the influence of external environmental factors on planktonic ecosystems, such as Salmon et al. (2020) and Nissen et al. (2021). However, there has been limited discussion on the seasonal variations in energy transfer within planktonic ecosystems, particularly the internal processes driving these dynamics. Therefore, this study focuses on the internal ecosystem dynamics, specifically examining the role of seasonal phytoplankton community succession in driving energy transfer to higher trophic levels.

However, challenges remain in accurately simulating the long-term impacts of rapid environmental changes, such as the recent decline in sea ice extent and potential shifts in ocean currents (Comiso et al., 2011; Parkinson, 2019; Turner et al., 2022; DuVivier et al., 2024). Kaufman et al. (2017) have used the Ross Sea ecological model MEDUSA to explore potential changes in phytoplankton community composition under climate change scenarios. However, there has been limited in-depth discussion on how climate change may alter internal energy transfer within the Ross Sea planktonic ecosystem, presumably due to the incomplete understanding of planktonic trophic

interactions. This study aims to provide insights into this issue. In future work, we plan to further investigate how these environmental changes alter phytoplankton succession and energy flow allocation, using sensitivity experiments to address these complexities and compensate for the limitations of *in-situ* observations.

4.3 *Impact of phytoplankton seasonal succession: universalism or endemicity*

For decades, the paradigm clash of plankton ecosystems between the high nutrient-low chlorophyll (HNLC) Southern Ocean and the productive Ross Sea has been a persistent concern (Martin, 1990; Smith and Asper, 2001; Smith et al., 2012; Wang et al., 2022; Mangoni et al., 2019). The seasonal succession of phytoplankton communities, particularly the transition, is not unique to the Ross Sea but is a widespread phenomenon observed across the Southern Ocean, including the Western Antarctic Peninsula (Arrigo et al., 2017; van Leeuwe et al., 2020; Joy-Warren et al., 2022), the Weddell Sea (Flynn et al., 2021), and the Amundsen Sea (Kwon et al., 2021). These studies highlight that light availability, iron dynamics, and mixed layer stability are common drivers of phytoplankton succession, with significant implications for zooplankton grazing strategies and energy flow pathways. For instance, diatoms are a preferred food source for Antarctic krill (*Euphausia superba*) due to their high nutritional value and digestibility, supporting efficient energy transfer to higher trophic levels (Smetacek et al., 2004; Schofield et al., 2017). In contrast, *Phaeocystis* colonies are less palatable and can form large blooms that are not efficiently consumed by grazers, leading to a decoupling of energy flow from primary producers to higher trophic levels (Schoemann et al., 2005; Smith and Kaufman, 2018). While the Ross Sea exhibits the most pronounced and well-studied succession pattern due to its unique hydrographic conditions and nutrient dynamics (Smith et al., 2014), the mechanisms underlying this phenomenon are broadly relevant to other Southern Ocean regions.

Currently, the ROSE model does not include krill as a functional group, despite its ecological importance. However, by adjusting the grazing preferences of mesozooplankton for diatoms, the model can be used to represent energy transfer pathways to higher trophic levels. In future work, we plan to develop a coupled framework linking the planktonic ecosystem with higher trophic levels, aiming to more realistically capture the characteristics of the Southern Ocean's biological hotspot represented by the Ross Sea. This will enable a deeper exploration of the mechanisms and spatiotemporal variations in energy transfer, thereby contributing to predictions of the Ross Sea ecosystem's potential responses to climate change.

5 Conclusions

Hindcast simulations of the three-dimensional regional ecosystem model ROSE reveal that dominant phytoplankton species in the Ross Sea vary seasonally, with diatoms (D) replacing *P. antarctica* (P) by late December. Correspondingly, zooplankton exhibits a similar seasonal succession, shifting from microzooplankton (Z) to mesozooplankton (M), with a time lag of over a month following the phytoplankton change. The formation and expansion of the RISP in austral spring and summer create favorable conditions for phytoplankton growth. However, as spring bloom depletes iron resources, the high-biomass area of plankton shifts southward toward the ice shelf front. Overall, P and Z show greater spatial variability in biomass compared to D and M.

In austral spring, P acts as the primary producer (the "P-period"), transferring 44% of the total phytoplankton energy loss to Z, six times the energy transfer to the larger zooplankton of M. In the austral summer, D becomes dominant and fuels M with greater efficiency than during the P-period. In this period, M obtains nearly half of the total phytoplankton energy loss, roughly 1.5 times that received by Z. The succession of phytoplankton communities enables an optimal period for upward energy transfer supported by D, enhancing energy transfer efficiency to top predators. This dynamic contributes to a long-lived, high-energy biological hotspot in the Ross Sea.

Given limited *in-situ* observations of zooplankton, this study provides valuable qualitative and quantitative insights into the ecological effects of seasonal phytoplankton succession on energy transfer using a three-dimensional regional ecosystem model. Recently, the seasonal succession of zooplankton along the Southern Ocean coast has gained attention (e.g., Garcia et al., 2020). As an "indicative area" experiencing polar warming, the Ross Sea study on plankton community composition and energy flow holds representative significance for exploring how trophic pyramids respond to climate change.

Acknowledgements

The authors are grateful to the NEMO and PISCES-v2 development team for providing the state-of-the-art model. The authors are grateful to Shuangling Chen, Walker O. Smith Jr., and Xiaolei Yu for making observed data on the Ross Sea shelf available (https://doi.org/10.1029/2021JC017749).

References

Ainley D G, Ballard G, Jones R, et al. 2015. Trophic cascades in the western Ross Sea, Antarctica: revisited. Marine Ecology Progress Series, 534: 1–16, doi: 10.3354/meps11394

Ainley D G, Jongsomjit D, Ballard G, et al. 2012. Modeling the relationship of Antarctic minke whales to major ocean boundaries. Polar Biology, 35(2): 281–290, doi: 10.1007/s00300-011-1075-1

Arndt S, Meiners K M, Ricker R, et al. 2017. Influence of snow depth and surface flooding on light transmission through Antarctic pack ice. Journal of Geophysical Research: Oceans, 122(3): 2108–2119, doi: 10.1002/2016JC012325

Arrigo K R, Robinson D H, Worthen D L, et al. 1999. Phytoplankton community structure and the drawdown of nutrients and CO_2 in the Southern Ocean. Science, 283(5400): 365–367, doi: 10.1126/science.283.5400.365

Arrigo K R, van Dijken G L. 2003. Phytoplankton dynamics within 37 Antarctic coastal polynya systems. Journal of Geophysical Research: Oceans, 108(C8): 3271

Arrigo K R, van Dijken G L, Alderkamp A C, et al. 2017. Early spring phytoplankton dynamics in the Western Antarctic Peninsula. Journal of Geophysical Research: Oceans, 122(12): 9350–9369, doi: 10.1002/2017JC013281

Arrigo K R, van Dijken G L, Bushinsky S. 2008. Primary production in the Southern Ocean, 1997–2006. Journal of Geophysical Research: Oceans, 113(C8): C08004

Atkinson A, Ward P, Hunt B P V, et al. 2012. An overview of Southern Ocean zooplankton data: abundance, biomass, feeding and functional relationships. CCAMLR Science, 19: 171–218

Aumont O, Ethé C, Tagliabue A, et al. 2015. PISCES-v2: an ocean biogeochemical model for carbon and ecosystem studies. Geoscientific Model Development, 8(8): 2465–2513, doi: 10.5194/gmd-8-2465-2015

Ballard G, Jongsomjit D, Veloz S D, et al. 2012. Coexistence of mesopredators in an intact polar ocean ecosystem: the basis for defining a Ross Sea marine protected area. Biological Conservation, 156: 72–82, doi: 10.1016/j.biocon.2011.11.017

Ballard G, Toniolo V, Ainley D G, et al. 2010. Responding to climate change: Adélie penguins confront astronomical and ocean boundaries. Ecology, 91(7): 2056–2069, doi: 10.1890/09-0688.1

Caron D A, Dennett M R, Lonsdale D J, et al. 2000. Microzooplankton herbivory in the Ross Sea, Antarctica. Deep-Sea Research Part Ⅱ: Topical Studies in Oceanography, 47(15–16): 3249–3272, doi: 10.1016/S0967-0645(00)00067-9

Chen S L, Smith W O Jr, Yu X L. 2021. Revisiting the ocean color algorithms for particulate organic carbon and chlorophyll-*a* concentrations in the Ross Sea. Journal of Geophysical Research: Oceans, 126(8): e2021JC017749, doi: 10.1029/2021JC017749

Christaki U, Gueneugues A, Liu Y, et al. 2021. Seasonal microbial food web dynamics in contrasting Southern Ocean productivity regimes. Limnology and Oceanography, 66(1): 108–122, doi: 10.1002/lno.11591

Cleary A C, Durbin E G, Casas M C. 2018. Feeding by Antarctic krill *Euphausia superba* in the West Antarctic Peninsula: differences between fjords and open waters. Marine Ecology Progress Series, 595: 39–54, doi: 10.3354/meps12568

Coale K H, Wang X J, Tanner S J, et al. 2003. Phytoplankton growth and biological response to iron and zinc addition in the Ross Sea and Antarctic circumpolar current along 170°W. Deep-Sea Research Part Ⅱ: Topical Studies in Oceanography, 50(3–4): 635–653, doi: 10.1016/S0967-0645(02)00588-X

Comiso J C, Kwok R, Martin S, et al. 2011. Variability and trends in sea ice extent and ice production in the Ross Sea. Journal of Geophysical Research: Oceans, 116(C4): C04021

Cristi A, Law C S, Pinkerton M, et al. 2024. Environmental driving forces and phytoplankton diversity across the Ross Sea region during a summer-autumn transition. Limnology and Oceanography, 69(4): 772–788, doi: 10.1002/lno.12526

Davis L S, Boersma P D, Court G S. 1996. Satellite telemetry of the winter migration of Adélie penguins (*Pygoscelis adeliae*). Polar Biology, 16(3): 221–225, doi: 10.1007/BF02329210

Davis L B, Hofmann E E, Klinck J M, et al. 2017. Distributions of krill and Antarctic silverfish and correlations with environmental variables in the western Ross Sea, Antarctica. Marine Ecology Progress Series, 584: 45–65, doi: 10.3354/meps12347

DuVivier A K, Molina M J, Deppenmeier A L, et al. 2024. Projections of winter polynyas and their biophysical impacts in the Ross Sea Antarctica. Climate Dynamics, 62(2): 989–1012, doi: 10.1007/s00382-023-06951-z

Elliott D T, Tang K W, Shields A R. 2009. Mesozooplankton beneath the summer sea ice in McMurdo Sound, Antarctica: abundance, species composition, and DMSP content. Polar Biology, 32(1): 113–122, doi: 10.1007/s00300-008-0511-3

El-Sayed S Z, Biggs D C, Holm-Hansen O. 1983. Phytoplankton standing crop, primary productivity, and near-surface nitrogenous nutrient fields in the Ross Sea, Antarctica. Deep-Sea Research Part A: Oceanographic Research Papers, 30(8): 871–886, doi: 10.1016/0198-0149(83)90005-5

Flynn R F, Bornman T G, Burger J M, et al. 2021. Summertime productivity and carbon export potential in the Weddell Sea, with a focus on the waters adjacent to Larsen C Ice Shelf. Biogeosciences, 18(22): 6031–6059, doi: 10.5194/bg-18-6031-2021

Garcia M D, Dutto M S, Chazarreta C J, et al. 2020. Micro- and mesozooplankton successions in an Antarctic coastal environment during a warm year. PLoS One, 15(5): e0232614, doi: 10.1371/journal.pone.0232614

Ge Y C, Zhang R F, Zhu Z Y, et al. 2024. Distributions of nutrients, trace metals, phytoplankton composition, and elemental consumption in the Ross and Amundsen Seas. Marine Chemistry, 265–266: 104436

Goetz K T. 2015. Movement, habitat, and foraging behavior of Weddell seals (*Leptonychotes weddellii*) in the western Ross Sea, Antarctica [dissertation]. Santa Cruz: University of California, 1–15

Haberman K L, Ross R M, Quetin L B. 2003. Diet of the Antarctic krill (*Euphausia superba Dana*): Ⅱ. Selective grazing in mixed phytoplankton assemblages. Journal of

Experimental Marine Biology and Ecology, 283(1–2): 97–113, doi: 10.1016/S0022-0981(02)00467-7

Hague M, Vichi M. 2021. Southern Ocean Biogeochemical Argo detect under-ice phytoplankton growth before sea ice retreat. Biogeosciences, 18(1): 25–38, doi: 10.5194/bg-18-25-2021

Hansen F C, van Boekel W H M. 1991. Grazing pressure of the calanoid copepod *Temora longicornis* on a *Phaeocystis* dominated spring bloom in a Dutch tidal inlet. Marine Ecology Progress Series, 78: 123–129, doi: 10.3354/meps078123

Jones R M, Smith W O Jr. 2017. The influence of short-term events on the hydrographic and biological structure of the southwestern Ross Sea. Journal of Marine Systems, 166: 184–195, doi: 10.1016/j.jmarsys.2016.09.006

Joy-Warren H L, Alderkamp A C, van Dijken G L, et al. 2022. Springtime phytoplankton responses to light and iron availability along the western Antarctic Peninsula. Limnology and Oceanography, 67(4): 800–815, doi: 10.1002/lno.12035

Katlein C, Perovich D K, Nicolaus M. 2016. Geometric effects of an inhomogeneous sea ice cover on the under-ice light field. Frontiers in Earth Science, 4: 6

Kaufman D E, Friedrichs M A M, Smith W O Jr, et al. 2017. Climate change impacts on southern Ross Sea phytoplankton composition, productivity, and export. Journal of Geophysical Research: Oceans, 122(3): 2339–2359., doi: 10.1002/2016JC012514

Kerkar A U, Venkataramana V, Tripathy S C. 2022. Assessing the trophic link between primary and secondary producers in the Southern Ocean: A carbon-biomass based approach. Polar Science, 31: 100734, doi: 10.1016/j.polar.2021.100734

Kooyman G L, Siniff D B, Stirling I, et al. 2004. Moult habitat, pre-and post-moult diet and post-moult travel of Ross Sea emperor penguins. Marine Ecology Progress Series, 267: 281–290, doi: 10.3354/meps267281

Kustka A B, Jones B M, Hatta M, et al. 2015. The influence of iron and siderophores on eukaryotic phytoplankton growth rates and community composition in the Ross Sea. Marine Chemistry, 173: 195–207, doi: 10.1016/j.marchem.2014.12.002

Kwon Y S, La H S, Jung J, et al. 2021. Exploring the roles of iron and irradiance in dynamics of diatoms and *Phaeocystis* in the Amundsen Sea continental shelf water. Journal of Geophysical Research: Oceans, 126(3): e2020JC016673, doi: 10.1029/2020JC016673

La H S, Lee H, Fielding S, et al. 2015. High density of ice krill (*Euphausia crystallorophias*) in the Amundsen sea coastal polynya, Antarctica. Deep-Sea Research Part Ⅰ: Oceanographic Research Papers, 95: 75–84, doi: 10.1016/j.dsr.2014.09.002

Leventer A, Dunbar R B. 1996. Factors influencing the distribution of diatoms and other algae in the Ross Sea. Journal of Geophysical Research: Oceans, 101(C8): 18489–18500, doi: 10.1029/96JC00204

Lindeman R L. 1942. The trophic-dynamic aspect of ecology. Ecology, 23(4): 399–417, doi: 10.2307/1930126

Madec G, NEMO Ocean Engine. 2008. Notes du Pôle de modélisation, Institut Pierre-Simon Laplace (IPSL), France, 1288–1619

Mangoni O, Saggiomo M, Bolinesi F, et al. 2019. *Phaeocystis antarctica* unusual summer bloom in stratified Antarctic coastal waters (Terra Nova Bay, Ross Sea). Marine Environmental Research, 151: 104733, doi: 10.1016/j.marenvres.2019.05.012

Mari X, Rassoulzadegan F, Brussaard C P D. 2004. Role of TEP in the microbial food web structure. Ⅱ. Influence on the ciliate community structure. Marine Ecology Progress Series, 279: 23–32, doi: 10.3354/meps279023

Martin J H. 1990. Glacial-interglacial CO_2 change: The iron hypothesis. Paleoceanography, 5(1): 1–13, doi: 10.1029/PA005i001p00001

McCain J S P, Allen A E, Bertrand E M. 2022. Proteomic traits vary across taxa in a coastal Antarctic phytoplankton bloom. The ISME Journal, 16(2): 569–579, doi: 10.1038/s41396-021-01084-9

Monti-Birkenmeier M, Diociaiuti T, Bolinesi F, et al. 2024. Microzooplankton and phytoplankton of Ross Sea polynya areas and potential linkage among functional traits. Deep-Sea Research Part Ⅱ: Topical Studies in Oceanography, 216: 105393, doi: 10.1016/j.dsr2.2024.105393

Nejstgaard J C, Tang K W, Steinke M, et al. 2007. Zooplankton grazing on *Phaeocystis*: a quantitative review and future challenges. Biogeochemistry, 83(1): 147–172

Nissen C, Vogt M. 2021. Factors controlling the competition between *Phaeocystis* and diatoms in the Southern Ocean and implications for carbon export fluxes. Biogeosciences, 18: 251–283, doi: 10.5194/bg-18-251-2021

Pakhomov E A, Perissinotto R. 1997. Spawning success and grazing impact of *Euphausia crystallorophias* in the Antarctic shelf region. In: Battaglia B, Valencia J, Walton D W H, eds. Antarctic Communities: Species, Structure and Survival. Cambridge: Cambridge University Press, 187–192

Parkinson C L. 2019. A 40-y record reveals gradual Antarctic sea ice increases followed by decreases at rates far exceeding the rates seen in the Arctic. Proceedings of the National Academy of Sciences of the United States of America, 116(29): 14414–14423

Peloquin J A, Smith W O Jr. 2007. Phytoplankton blooms in the Ross Sea, Antarctica: Interannual variability in magnitude, temporal patterns, and composition. Journal of Geophysical Research: Oceans, 112(C8): C08013

Pinkerton M H, Forman J, Bury S J, et al. 2013. Diet and trophic niche of Antarctic silverfish *Pleuragramma antarcticum* in the Ross Sea, Antarctica. Journal of Fish Biology, 82(1): 141–164, doi: 10.1111/j.1095-8649.2012.03476.x

Rousset C, Vancoppenolle M, Madec G, et al. 2015. The Louvain-La-Neuve sea ice model LIM3.6: Global and regional capabilities. Geoscientific Model Development, 8(10): 2991–3005, doi: 10.5194/gmd-8-2991-2015

Ryan-Keogh T J, Smith W O Jr. 2021. Temporal patterns of iron limitation in the Ross Sea as determined from chlorophyll fluorescence. Journal of Marine Systems, 215: 103500, doi: 10.1016/j.jmarsys.2020.103500

Ryderheim F, Hansen P J, Kiørboe T. 2022. Predator field and colony morphology determine the defensive benefit of colony formation in marine phytoplankton. Frontiers in Marine Science, 9: 829419, doi: 10.3389/fmars.2022.829419

Sala A, Azzali M, Russo A. 2002. Krill of the Ross Sea: distribution, abundance and demography of Euphausia superba and Euphausia crystallorophias during the Italian Antarctic Expedition (January-February 2000). Scientia Marina, 66(2): 123–133, doi: 10.3989/scimar.2002.66n2123

Salmon E, Hofmann E E, Dinniman M S, et al. 2020. Evaluation of iron sources in the Ross Sea. Journal of Marine Systems, 212: 103429, doi: 10.1016/j.jmarsys.2020.103429

Schmidt K, Schlosser C, Atkinson A, et al. 2016. Zooplankton gut passage mobilizes lithogenic iron for ocean productivity. Current Biology, 26(19): 2667–2673, doi: 10.1016/j.cub.2016.07.058

Schoemann V, Becquevort S, Stefels J, et al. 2005. *Phaeocystis* blooms in the global ocean and their controlling mechanisms: a review. Journal of Sea Research, 53(1–2): 43–66, doi: 10.1016/j.seares.2004.01.008

Schofield O, Saba G, Coleman K, et al. 2017. Decadal variability in coastal phytoplankton community composition in a changing West Antarctic Peninsula. Deep Sea Research Part Ⅰ: Oceanographic Research Papers, 124: 42–54, doi: 10.1016/j.dsr.2017.04.014

Sedwick P N, Garcia N S, Riseman S F, et al. 2007. Evidence for high iron requirements of colonial *Phaeocystis antarctica* at low irradiance. Biogeochemistry, 83(1): 83–97

Sedwick P N, Marsay C M, Sohst B M, et al. 2011. Early season depletion of dissolved iron in the Ross Sea polynya: implications for iron dynamics on the Antarctic continental shelf. Journal of Geophysical Research: Oceans, 116(C12): C12019, doi: 10.1029/2010JC006553

Shields A R, Smith Jr W O. 2008. An examination of the role of colonial *Phaeocystis antarctica* in the microbial food web of the Ross Sea. Polar Biology, 31(9): 1091–1099, doi: 10.1007/s00300-008-0450-z

Smetacek V, Assmy P, Henjes J. 2004. The role of grazing in structuring Southern Ocean pelagic ecosystems and biogeochemical cycles. Antarctic Science, 16(4): 541–558, doi: 10.1017/S0954102004002317

Smith W O Jr. 2022. Primary productivity measurements in the Ross Sea, Antarctica: A regional synthesis. Earth System Science Data, 14(6): 2737–2747, doi: 10.5194/essd-14-2737-2022

Smith W O Jr, Ainley D G, Arrigo K R, et al. 2014. The oceanography and ecology of the Ross Sea. Annual Review of Marine Science, 6: 469–487, doi: 10.1146/annurev-marine-010213-135114

Smith W O Jr, Ainley D G, Cattaneo-Vietti R. 2007. Trophic interactions within the Ross Sea continental shelf ecosystem. Philosophical Transactions of the Royal Society B: Biological Sciences, 362(1477): 95–111, doi: 10.1098/rstb.2006.1956

Smith W O Jr, Asper V L. 2001. The influence of phytoplankton assemblage composition on biogeochemical characteristics and cycles in the southern Ross Sea, Antarctica. Deep-Sea Research Part Ⅰ: Oceanographic Research Papers, 48(1): 137–161, doi: 10.1016/S0967-0637(00)00045-5

Smith W O Jr, Comiso J C. 2008. Influence of sea ice on primary production in the Southern Ocean: A satellite perspective. Journal of Geophysical Research: Oceans, 113(C5): C05S93

Smith W O Jr, Delizo L M, Herbolsheimer C, et al. 2017. Distribution and abundance of mesozooplankton in the Ross Sea, Antarctica. Polar Biology, 40(12): 2351–2361, doi: 10.1007/s00300-017-2149-5

Smith W O Jr, Dinniman M S, Tozzi S, et al. 2010. Phytoplankton photosynthetic pigments in the Ross Sea: patterns and relationships among functional groups. Journal of Marine Systems, 82(3): 177–185, doi: 10.1016/j.jmarsys.2010.04.014

Smith W O Jr, Kaufman D E. 2018. Climatological temporal and spatial distributions of nutrients and particulate matter in the Ross Sea. Progress in Oceanography, 168: 182–195, doi: 10.1016/j.pocean.2018.10.003

Smith W O Jr, Meyer M G. 2020. Marine plankton of open Antarctic seas. In: Goldstein M I, DellaSala D A, eds. Encyclopedia of the World's Biomes. Netherlands: Elsevier, 623–634

Smith W O Jr, Nelson D M, DiTullio G R, et al. 1996. Temporal and spatial patterns in the Ross Sea: phytoplankton biomass, elemental composition, productivity and growth rates. Journal of Geophysical Research: Oceans, 101(C8): 18455–18465, doi: 10.1029/96JC01304

Smith W O Jr, Sedwick P N, Arrigo K R, et al. 2012. The Ross Sea in a sea of change. Oceanography, 25(3): 90–103, doi: 10.5670/oceanog.2012.80

Smith W O Jr, Shields A R, Peloquin J A, et al. 2006. Interannual variations in nutrients, net community production, and biogeochemical cycles in the Ross Sea. Deep-Sea Research Part Ⅱ: Topical Studies in Oceanography, 53(8–10): 815–833, doi: 10.1016/j.dsr2.2006.02.014

Smith W O Jr, Tozzi S, Long M C, et al. 2013. Spatial and temporal variations in variable fluoresence in the Ross Sea (Antarctica): oceanographic correlates and bloom dynamics. Deep-Sea Research Part Ⅰ: Oceanographic Research Papers, 79: 141–155, doi: 10.1016/j.dsr.2013.05.002

Steinberg D K, Landry M R. 2017. Zooplankton and the ocean carbon cycle. Annual review of marine science, 9(1): 413–444, doi: 10.1146/annurev-marine-010814-015924

Strzepek R F, Hunter K A, Frew R D, et al. 2012. Iron-light interactions differ in Southern Ocean phytoplankton. Limnology and Oceanography, 57(4): 1182–1200, doi: 10.4319/lo.2012.57.4.1182

Tagliabue A, Arrigo K R. 2003. Anomalously low zooplankton

abundance in the Ross Sea: An alternative explanation. Limnology and Oceanography, 48(2): 686–699, doi: 10.4319/lo.2003.48.2.0686

Tang K W, Smith W O Jr, Elliott D T, et al. 2008. Colony size of *Phaeocystis antarctica* (Prymnesiophyceae) as influenced by zooplankton grazers. Journal of Phycology, 44(6): 1372–1378, doi: 10.1111/j.1529-8817.2008.00595.x

Thrush S, Dayton P, Cattaneo-Vietti R, et al. 2006. Broad-scale factors influencing the biodiversity of coastal benthic communities of the Ross Sea. Deep Sea Research Part Ⅱ: Topical Studies in Oceanography, 53(8–10): 959–971, doi: 10.1016/j.dsr2.2006.02.006

Turner J, Holmes C, Caton Harrison T, et al. 2022. Record low Antarctic sea ice cover in February 2022. Geophysical Research Letters, 49(12): e2022GL098904, doi: 10.1029/2022GL098904

Vancoppenolle M, Fichefet T, Goosse H, et al. 2009. Simulating the mass balance and salinity of Arctic and Antarctic sea ice. 1. Model description and validation. Ocean Modelling, 27(1–2): 33–53, doi: 10.1016/j.ocemod.2008.10.005

van Leeuwe M A, Webb A L, Venables H J, et al. 2020. Annual patterns in phytoplankton phenology in Antarctic coastal waters explained by environmental drivers. Limnology and Oceanography, 65(7): 1651–1668, doi: 10.1002/lno.11477

Wang T J, Wei H, Xiao J G. 2022. Dynamic linkage between the interannual variability of the spring Ross Ice Shelf Polynya and the atmospheric circulation anomalies. Climate Dynamics, 58(3): 831–840

Weisse T, Tande K, Verity P, et al. 1994. The trophic significance of *Phaeocystis* blooms. Journal of Marine Systems, 5(1): 67–79, doi: 10.1016/0924-7963(94)90017-5

Woodward F I. 2007. Global primary production. Current Biology, 17(8): R269–R273, doi: 10.1016/j.cub.2007.01.054

Wu Miao, McCain J S P, Rowland E, et al. 2019. Manganese and iron deficiency in Southern Ocean *Phaeocystis antarctica* populations revealed through taxon-specific protein indicators. Nature Communications, 10(1): 3582, doi: 10.1038/s41467-019-11426-z

Zhang Yimin, Yang Wei, Zhao Wei, et al. 2023a. Spatial and seasonal variations of near-inertial kinetic energy in the upper Ross Sea and the controlling factors. Frontiers in Marine Science, 10: 1173900, doi: 10.3389/fmars.2023.1173900

Zhang Yongli, Zhao Wei, Wei Hao, et al. 2023b. Iron limitation and uneven grazing pressure on phytoplankton co-lead the seasonal species succession in the Ross Ice Shelf Polynya. Journal of Geophysical Research: Oceans, 128(3): e2022JC019026, doi: 10.1029/2022JC019026

Zhang Yongli. 2024. Modelling and mechanism analysis on spatio-temporal characteristics of phytoplankton over the Ross Sea Shelf (in Chinese) [dissertation]. Tianjin: Tianjin University. https://doi.org/10.6084/m9.figshare.29481020.v1

Supplementary information:

Table S1. References on trophic interactions, habitat distribution, and migration pathways among major species in the Ross Sea.

Table S2. Data sources of forcing fields, initial conditions and open boundary used by ROSE simulation covering 2010−2020.

The supplementary information is available online at https://doi.org/10.1007/s13131-025-2477-1 and http://www.aosocean.com/. The supplementary information is published as submitted, without typesetting or editing. The responsibility for scientific accuracy and content remains entirely with the authors.

Appendix

Table A1. List of English abbreviations

Abbreviation	Full name	Abbreviation	Full name
1. Geographic name			
A2C	Aviator Ice Tongue to Coulman Island	HoB	Houtz Bank
AIT	Aviator Ice Tongue	IB	Iselin Bank
ASL	Amundsen Sea Low	JT	Joides Trough
CA	Cape Adare	MB	Mawson Bank
CB	Crary Bank	MMS	McMurdo Sound
CCb	Cape Colbeck	NIB	Northern of Iselin Bank
CI	Coulman Island	PB	Pennell Bank
DIT	Drygalski Ice Tongue	RB	Ross Bank
DT	Drygalski Trough	RI	Ross Island
E7L	Edward Ⅶ Land	RS	Ross Sea
ESLF	Eastern Shelf	SO	Southern Ocean
ESLP	Eastern Slope	SPB	Southern of Pennell Bank
GCT	Glomar Challenger Trough	VL	Victoria Land
HaB	Hayes Bank		
2. Terms of ice shelf, polynyas and hydrography			
AABW	Antarctic bottom water	RG	Ross Gyre
ACC	Antarctic circumpolar current	RIS	Ross Ice Shelf
ASC	Antarctic slope current	RISP	Ross Ice Shelf polynya
CDW	Circumpolar deep water	TNBP	Terra Nova Bay polynya
3. Terms of southern ocean conservation area			
CCAMLR	the commission for the conservation of Antarctic marine living resources	RMP	Research and monitoring plan
GPZ	General protection zone	SRZ	Special research zone
KRZ	Krill research zone		